Tech. Bull. Fac. Agr. Kagawa Univ. Vol. 38, No. 1, 25～36, 1986

深浦養魚場における養殖ハマチの許容漁場容量評価に関する研究 (III)

深浦湾における潮流の数値計算

佐々木 孝，ポタピロム・ティーカウス，井上 裕雄

STUDIES ON THE ASSESSMENT OF THE ALLOWABLE STOCKING CAPACITY OF YELLOWTAIL CULTURED IN THE FUKAURA FISH FARM (III)

Numerical investigations on the tidal current in the Fukaura-wan

Takashi SASAKI, Teekawuth POTAPIROM* and Hiroo INOUE

若松瀬戸南部に位置する深浦湾には二つの湾口部があり，その北側湾口部の開口部は250 m であり，水深は19 m 程度である．湾口付近には多数の養殖網生簀がある．湾奥部がもう一つの南側湾口部と幅9.2 m 程の狭水道で結合されている．底質は細砂が主であり，湾口部は粗砂である．深浦湾の地形的および湾内の特徴を考慮して，湾内および湾近傍の潮流計算を実施した．解析領域は前報の MODEL I の内部にとり，MODEL I で得られた結果を初期条件および境界条件とした MODEL II を使って潮流シミュレーションをすすめた．特に湾奥の狭水道の存在，海底摩擦抵抗および湾口部における網生簀の流れに対する影響などについて研究した．結果は観測データとよく適合した．また最終的に得られた潮流場をもとに計算された海水交流率が12時間当り5.6となることが認められた．

Fukaura-wan with two bay mouths is connected to the main stream in the southern part of Wakamatsu-seto. The northern mouth of the bay is about 250 m wide and about 19 m deep. There are a number of culture cages near this mouth. The southern mouth located at the bay bottom is opened to the main stream by a channel which divides into two branch channels. The channel is 9.2 m wide at high tide. The sediment of the bay is composed of fine sand except near the northern mouth where sediment is composed of coarse sand.

Taking into account the features stated above, we proceeded to make numerical calculations of the tidal currents in and near the bay.

The computed area of MODEL II, 2.6 km long in the N–S direction and 1.6 km wide in the E–W direction, was taken within MODEL I. The grid point interval is 50 m and time step is 3.0 sec. The sea level variations on both boundaries and the initial currents in the area were those obtained by computations on MODEL I.

We calculaled the effects of narrow channel, bottom friction, and interaction of culture net cages and currents.

The results computed were in good agreement with the observed data. It was also found that if the volume of inflow from the main mouth of the bay was Q_{in} and the water volume at L.W. was V_l, then the exchange rate of sea water, Q_{in}/V_l, was 5.6 in 1/12 hrs.

Introduction

In the previous paper, we analyzed the tidal current data observed in and out of Fukaura-wan and then we made a

* Kasetsart University, Bangkok, Thailand

numerical calculation of the tidal currents in and around Wakamatsu-seto including Fukaura-wan from the macroscopic standpoint, as solved in MODEL I. Consequently, we made clear the hydraulic characteristics of the main stream of Wakamatsu-seto.

In this report, the computations of tidal currents were performed on a fine grid model located within MODEL I, referred to in this paper as MODEL II, because it is essential for subsequent water quality analysis and ecological simulation to understand the features of sea water flows in and near Fukaura-wan in detail.

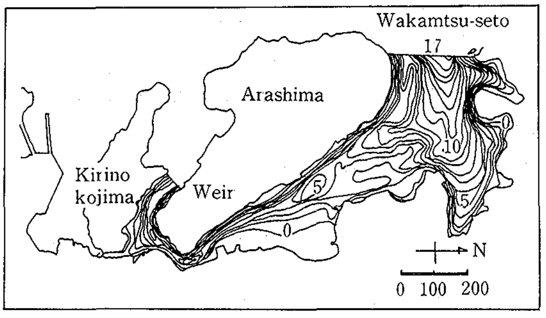

Fig 1. Geometry and bottom topography in Fukaura-wan.

Fukaura-wan with two bay mouths is connected to the main stream in the southern part of Wakamatsu-seto. The northern mouth of the bay is about 250 m wide and about 19 m deep. There are a number of culture cages near this main mouth. The southern mouth located at the bay bottom is opened to the main stream by a channel which divides into two branch channels. The channel is 9.2 m wide at high tide (Fig. 1). The bottom sediment of the bay is composed of fine sand except near the northern mouth where the sediment is composed of coarse sand.

Taking into account the features stated above, we proceeded to make numerical calculations of the tidal currents in and near the bay.

Method

The computed area of MODEL II, 2.6 km long in the N−S direction and 1.6 km wide in the E−W direction, was taken within MODEL I. The grid point interval is 50 m and time step is 3.0 sec. The sea level variations on both boundaries and the initial currents in the area were those obtained by computations on MODEL I (Figs. 2−4).

At first, we checked the effects of narrow channel, bottom friction and culture net cages floated.

The effect of narrow channel

Fukaura-wan has four contracted cross sections in the form of a channel which divides into two branch channels and a weir as shown in Fig. 1. The branch channels are 25 m and 7 m in width, respectively. The weir consists of three rectangular orifices of 2 m in width with a crest level of 1.06 m at low tide. It is not cost-effective to use a grid as small as the actual cross sectional width or less. However, neither is it accurate to extend artificially the narrow width to one grid interval nor to reduce the water depth to maintain the same cross sectional area.

Therefore, we have expressed the cross section less than one grid interval as follows:

$$\Delta s_{i,j} = \alpha_{i,j} \Delta s \tag{1}$$

where $\alpha_{i,j}$ is the contraction ratio, $\Delta s_{i,j}$ the width of the narrow channel and Δs the grid interval.

The equation of continuity, with the contraction ratio, may be transformed into the following finite-difference equation.

$$\zeta^{t+1}_{i,j} = \zeta^{t-1}_{i,j} - X^{t}_{i+1,j}\alpha_{i+1,j} + X^{t}_{i-1,j}\alpha_{i-1,j} - Y^{t}_{i,j+1}\alpha^{t}_{i,j+1} + Y^{t}_{i,j-1}\alpha^{t}_{i,j-1} \tag{2}$$

where $\alpha_{i+1,j}$, $\alpha_{i-1,j}$, $\alpha_{i,j-1}$ and $\alpha_{i,j+1}$ are the contraction ratios of left, right, bottom and top side of grid point (i, j) respectively, X the discharge in the x-direction, Y the discharge in the y-direction and ζ the fluctuation from the mean sea level.

Eq. (2) is applied to the grid point in regions A and B of two branch channels (Fig. 5(A)).

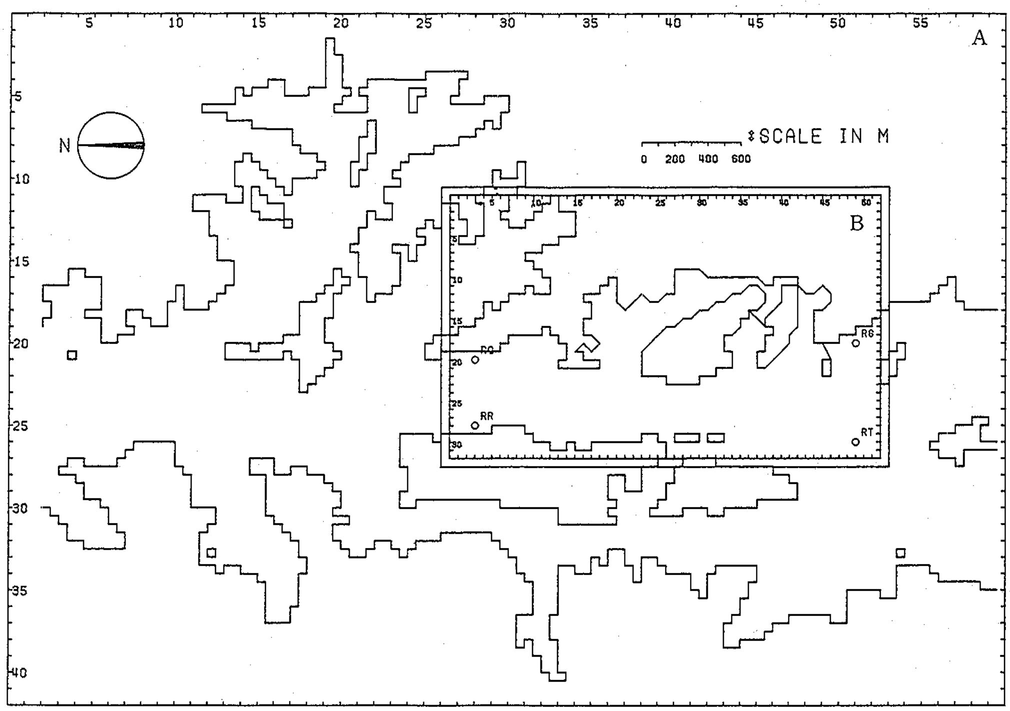

Fig. 2 Computed areas of MODEL I and MODEL II; A: MODEL I, B: MODEL II.

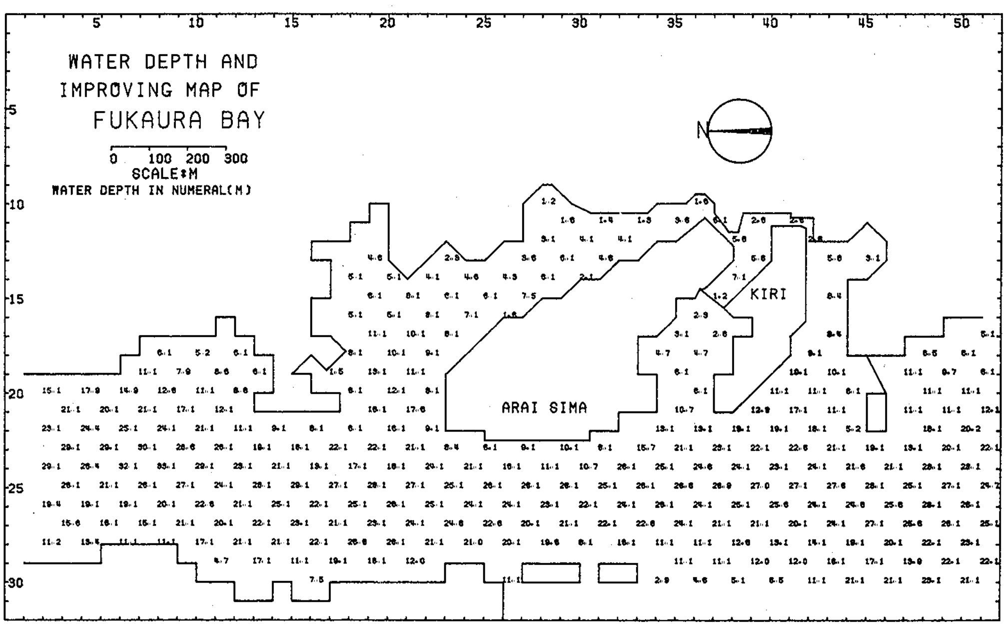

Fig. 3 Water depth in and near Fukaura-wan at L.W.

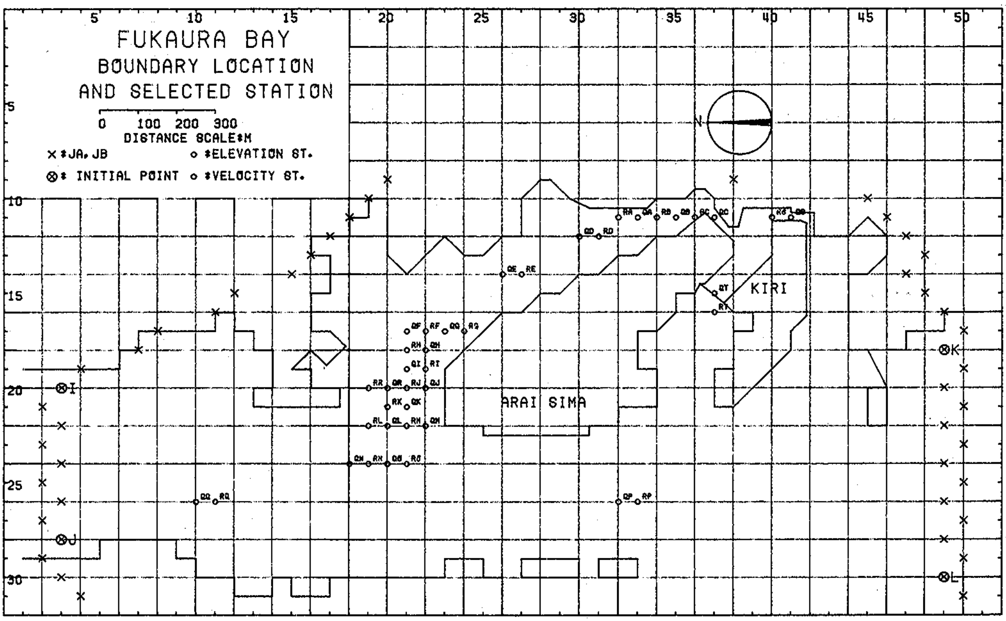

Fig. 4. Analysis-area for the finite-difference method with square meshes. RA～RT: monitoring stations of tidal elevation. QA～QT: monitoring stations of tidal current. I～L: boundary location.

The influence of bottom friction

The internal friction is too insignificant to be considered in calculations of the long wave, so only bottom friction is considered here. The coefficient of sea bottom friction, γ^2, depends on the roughness of the bottom. In the deeper seas the value changes as depth decreases. In the case of Fukaura-wan, we will use different values of γ^2 in main flow, bay and narrow channel, respectively.

An analogous effect is found in the Manning's formula, which is usually applied in hydraulic engineering involving open channel flow.

The Chézy's constant may be written by using the Manning's roughness parameter as follows

$$C=m^{1/6}/n, \quad \gamma^2=gC^{-2} \tag{3}$$

where m is the hydraulic radius and equals to A/P, A the cross-sectional area, P the wetted perimeter of the cross section, C the Chézy's constant and n the Manning's roughness parameter.

The values of n have been determined for various kinds of bed materials and type of channels. If the value of Manning's n is given, we can estimate the coefficient of sea bottom friction, γ^2, from Eq. (3).

The interaction of culture net cages and currents

There are a number of culture net cages near the main mouth located at the northern part of Fukaura-wan. The total surface area of the cages is about 10% of the total bay area (0.26 km^2). The depth of the bay is shallow. The effect of currents on net cages creates as the external force. Accordingly, in the momentum equations we must take into account the external force due to the fish cages, i.e. the drag vector components, (K_x, K_y, g), where K_x and K_y are the drag force per unit volum in x- and y- directions, respectively.

The drag force on the net is expressed as follows[(3)].

$$F=\lambda C_D \rho_w (d/s)\, V^2 \tag{4}$$

where F is the drag force on the net, λ the interference coefficient between net strings, C_D the coefficient of drag on

Table 1 The conditions of each model in studies on the influences of bottom friction, narrow channel, and the interaction of net cages and currents

Model No.	Conditions
II−1	Bottom friction estimated by using Manning's parameter was constant ($\gamma^2=0.0065$) and equal to that in the main flow outside the bay. Effects of narrow channels in regions A and B were not considered (see Fig. A)
II−2	Bottom friction estimated by using Manning's parameter was constant ($\gamma^2=0.0065$) and equal to that in the main flow outside the bay. Effects of narrow channels in regions A and B were considered by using the contraction ratio method (see Fig. B)
II−3	Effects of narrow channels in regions A and B were considered by using the contraction ratio method (see Fig. B). Bottom frictions γ^2 were 0.0065 in the main flow, 0.0195 in the bay, 0.0617 in region A and 0.0357 in region B, respectively. (see Fig. D)
II−4	Effects of narrow channels in regions A and B were considered by using the contraction ratio method (see Fig. B). Bottom frictions γ^2 were 0.0065 in the main flow, 0.0195 in the bay, 0.0617 in region A and 0.0357 in region B, respectively. (see Fig. D). The interaction of net cages and currents in the net cages region (see Fig C) was considered

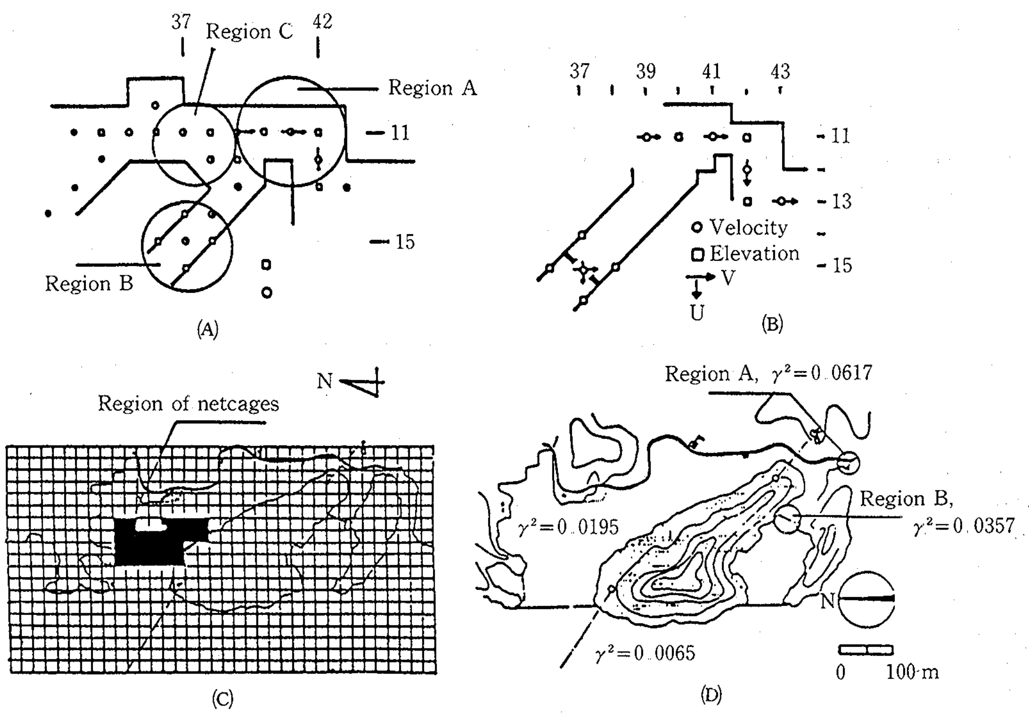

Fig. 5 Schematic models.

the net, ρ_w the mass density of sea water, d the diameter of the string, s the nominal mesh size, and V the velocity.

All net cages are rearranged near the northern bay mouth so that the sum of each peripheric length of them set in some grids is equivalent to the total length of sides of the grids. In such a case, it may be assumed that the nets are put up along all sides of the grids.

The grids painted black, as shown in Fig. 5(C), are the area where the net cages are tentatively set in the sense mentioned above.

Integrating the external force term with respect to z, we obtain

$$\int_{-\zeta}^{h}(K_x)dz=(h+\zeta)\bar{K}_x \qquad \int_{-\zeta}^{h}(K_y)dz=(h+\zeta)\bar{K}y \tag{5}$$

Considering the assumption mentioned above and substituting Eq. (4) into Eq. (5), with $\lambda=1$ and C_D=constant, we obtain

$$\int_{-\zeta}^{h}(K_x)dz/(h+\zeta)=-C_D(d/s)\,U\,(U^2+V^2)^{\frac{1}{2}}\,L/(\Delta s(h+\zeta)) \qquad \int_{-\zeta}^{h}(K_y)dz/(h+\zeta)=-C_D(d/s)\,V\,(U^2+V^2)^{\frac{1}{2}}\,L/(\Delta s(h+\zeta)) \tag{6}$$

where L is the depth of the fishing net, Δs the grid interval, U and V the vertically averaged velocities with respect to x- and y- directions, respectively, h the elevation of the bottom with respect to mean sea level and ζ the elevation of water surface with respect to mean sea level. Eq. (6) may be rewritten as

$$\int_{-\zeta}^{h}(K_x)dz=-C_D(d/s)(L/\Delta s)\,M\,(U^2+V^2)^{\frac{1}{2}} \qquad \int_{-\zeta}^{h}(K_y)dz=-C_D(d/s)(L/\Delta s)\,N\,(U^2+V^2)^{\frac{1}{2}} \tag{7}$$

where M and N are the discharge with respect to x- and y- directions, respectively.

The equations of momentum including the interaction of culture net cages and currents are

$$\frac{\partial M}{\partial t}=-\left[\left\{\frac{C_D(d/s)(L/\Delta s)+\gamma^2}{(h+\zeta)}\right\}\sqrt{U^2+V^2}+2\frac{\partial U}{\partial x}+\frac{\partial U}{\partial Y}+\frac{U}{(h+\zeta)}\frac{\partial(h+\zeta)}{\partial x}\right]M$$

Table 2. The parameters reltated to the computer simulation

description	unit	symbol	spring tide	neap tide
time interval	second	Δt	3	3
grid interval	cm.	Δs	10000.	10000.
Corioli's force	1/sec.	f	.00007893	.00007893
wave angular frequency due to moon	deg/hr.	δ	28.9841	28.9841
horizontal eddy viscosity	cm^2/sec	A_l	2700.	2700.
gravitational acceleration	cm^2/sec	g	980.	980.
nondimensional frictional constant		γ^2		
Wakamatsu Strait			0.0065	0.0065
Fukaura Bay			0.0195	0.0195
mass density of sea water	g/cm^3	ρ_ω	1.025	1.025
drag coefficient of netting		C_D	4	4
coefficient of interference		λ	1	1
ratio of twine diameter to nominal mesh size		d/s	0.4	0.4
initial tide at boundary point	cm.	I	15.42	7.72
		J	15.42	7.72
		K	28.71	14.36
		L	28.71	14.36

$$+\left\{f-\frac{\partial U}{\partial y}-\frac{U}{(h+\zeta)}\frac{\partial(h+\zeta)}{\partial x}\right\}N-g(h+\zeta)\frac{\partial\zeta}{\partial x}$$

$$\frac{\partial N}{\partial t}=-\left[\left\{\frac{C_D(d/s)(L/\Delta s)+\gamma^2}{(h+\zeta)}\right\}\sqrt{U^2+V^2}+2\frac{\partial V}{\partial y}+\frac{\partial U}{\partial x}+\frac{V}{(h+\zeta)}\frac{\partial(h+\zeta)}{\partial y}\right]N \qquad (8)$$

$$+\left\{f-\frac{\partial V}{\partial x}-\frac{V}{(h+\zeta)}\frac{\partial(h+\zeta)}{\partial y}\right\}M-g(h+\zeta)\frac{\partial\zeta}{\partial y}$$

where f is the Corioli's force parameter and g the gravitational acceleration.

Numerical caculations on the tidal currents were performed for the conditions shown in Table 1 and Table 2.

Results and discussion

a. The influence of the narrow channel, the bottom friction and the interaction of culture net cages and currents

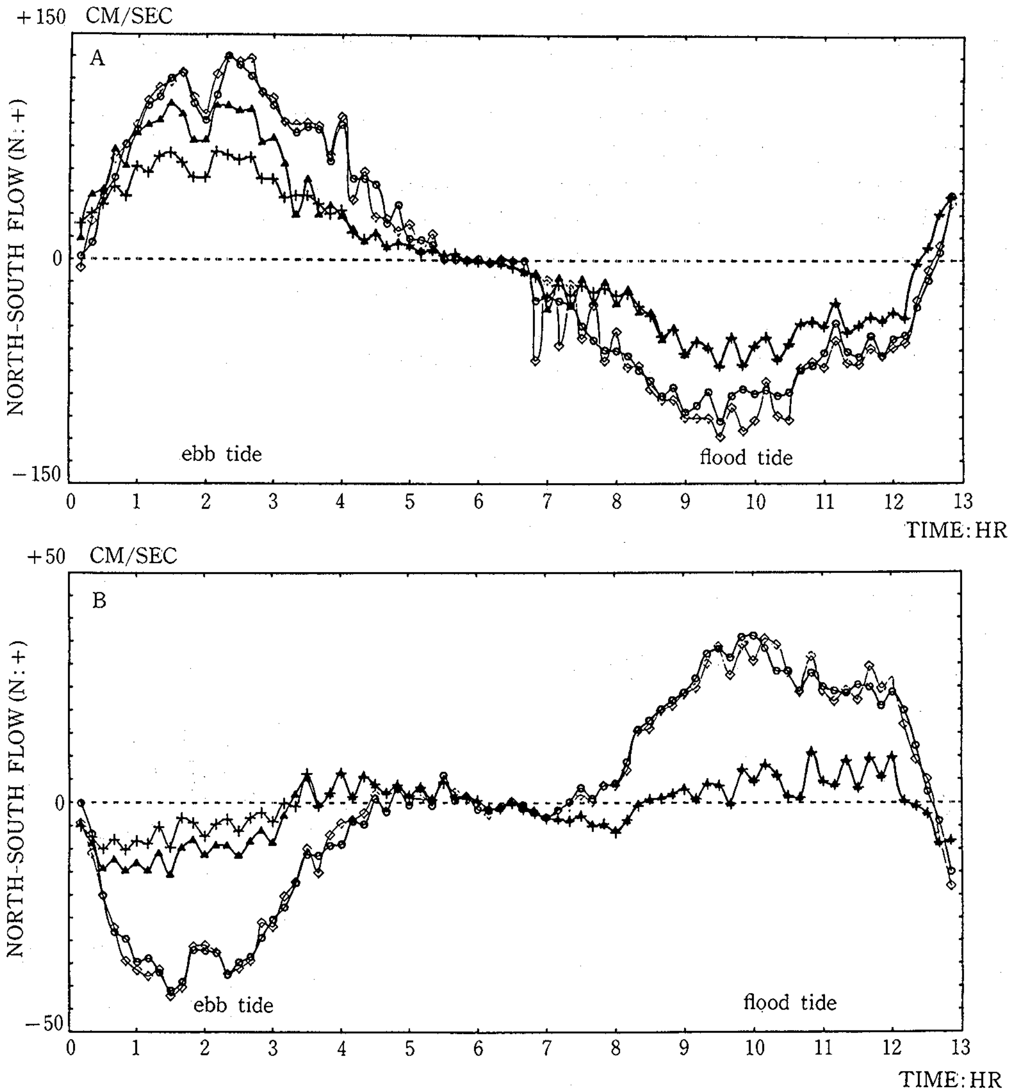

Fig. 6 Comparison of each condition in MODEL II, Spring tide. A: monitoring station QT (15, 37), B: monitoring station QB (11, 35), ○: MODEL II−1, ◇: MODEL II−2, △: MODEL II−3, +: MODEL II−4

Four different models were made and compared with each other. The conditions of each model are shown in Fig. 5 and Table 1.

In regions A and B, the formula for the narrow channels was applied. At the channel C we applied the equivalent depth method because the axis of the channel inclined toward the axis of the model, and the coefficient of sea bottom friction was determined by considering $n=0.045$ as used in the case of natural rough wall streams.

After running tests were practiced on MODEL II under the conditions as shown in Table 1, the coefficient of sea bottom friction, γ^2, and the contracted section ratio, α, were estimated to be as follows.

In the main flow	$\gamma^2=0.0065$
In the bay	$\gamma^2=0.0195$
In the narrow channel	
Region A	$\gamma^2=0.0617$
Region B	$\gamma^2=0.0357$
	$\alpha=0.5$

In these running tests, it was found that in Fukaura-wan the effect of bottom friction upon the tidal currents was fairly sensitive.

Using Eq. (8), we investigated on the interaction of culture net cages and currents in the bay. The area of culture net cages examined is shown in Fig. 5. We used the value of C_D in fouled netting obtained by Milne[4]. The result computed is shown in Fig. 6. From this figure, we found that the influence of drag force on net cages was significent during ebb tide only. At ebb tide sea water flows into Fukaura-wan through the northern bay mouth and flows out through the southern bay mouth. Since the culture net cages located near the main northern mouth receive extremely fast currents from the main stream of Wakamatsu-seto, the interaction of culture net cages and currents at the bay mouth becomes strong enough to decrease the current speeds in the bay. On the other hand, during flood tide their interaction is weak due to the sea water being stagnant near the bay mouth.

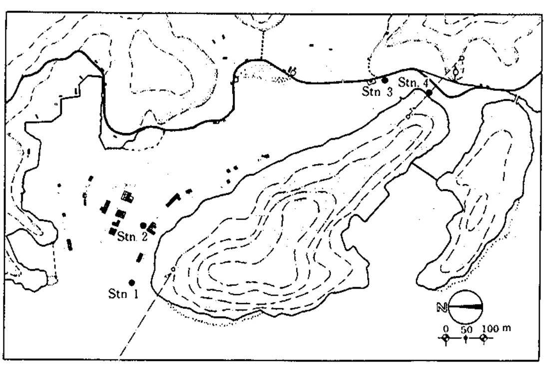

Fig. 7. Map showing the location of observation stations and culture net cages.

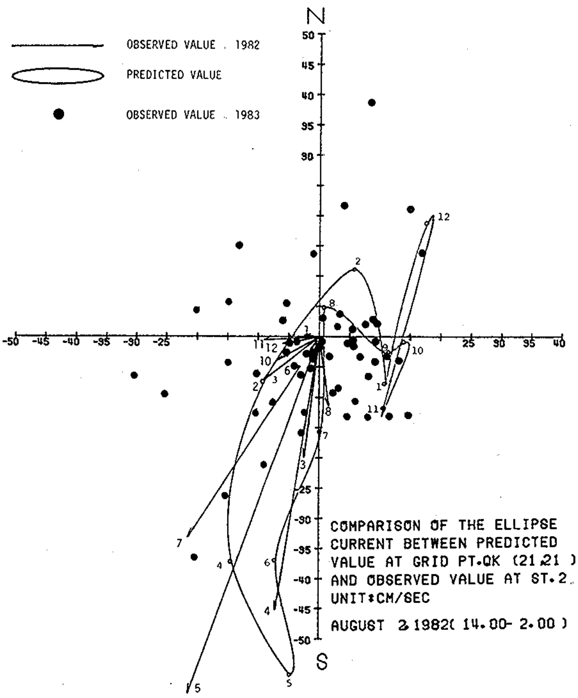

Fig. 8. Comparison of observed and computed tidal currents.

b. The reliabilty of the simulation model

Comparison of computed values with the actual observed values is necessary for checking the reliability of the simulation model. The monitoring stations for checking are shown in Fig. 4. At each station shown in Fig. 7, tidal currents were measured at 2−3 m below the surface.

Fig. 8 shows the computed values of tidal currents at a monitoring station, $QK(i=21, j=21)$, during neap tide. Actual measured currents, obtained on August 2, 1982, were superimposed on this figure and good agreement was

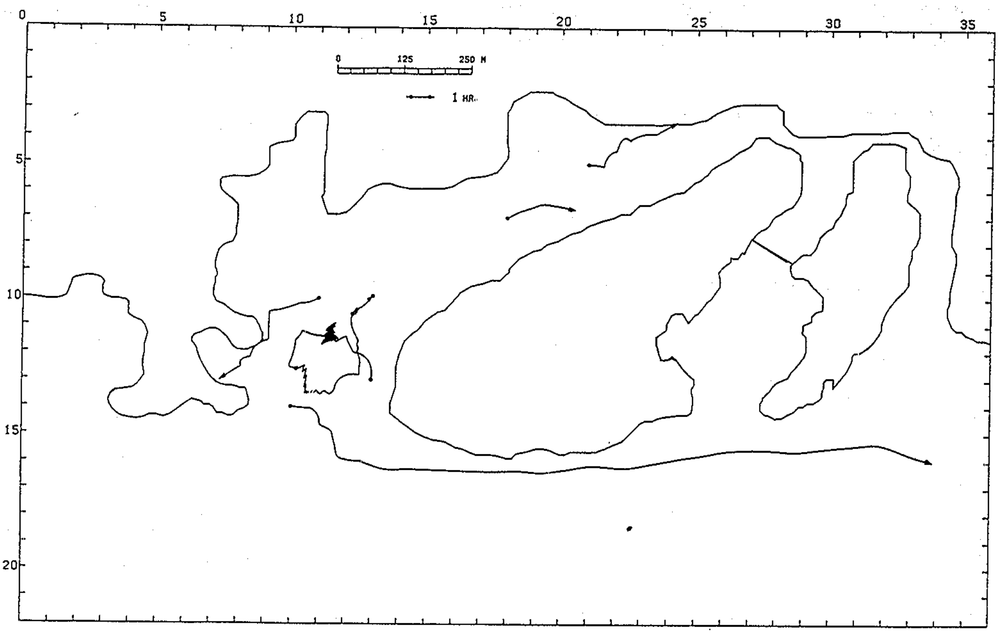

Fig. 9 Computed trajectories of drifters (water mass).

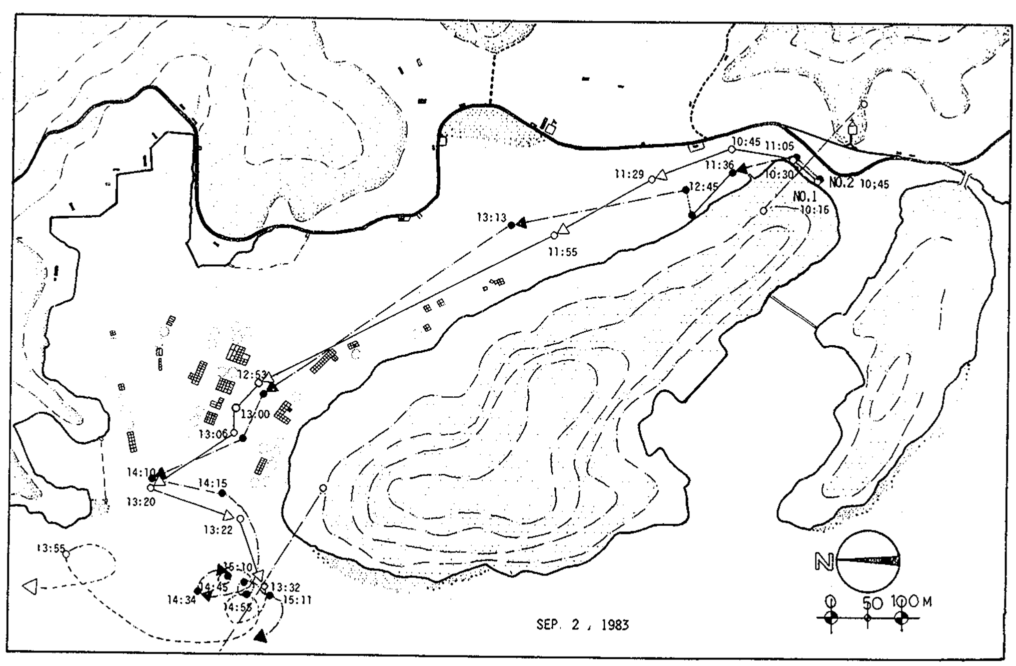

Fig. 10 Observed trajectories of drifters.

seen between the computed and measured currents.

Using the distribution of currents obtained on MODEL II−4, we checked Lagrangian movement of water mass over the tidal cycle as shown in Fig. 9. It can be seen that drifter trajectories obtained by field observations were similar to those computed, from a macroscopic standpoint (Fig. 10). The estimated discharge at the contracted narrow channel on MODEL II−4 coincided for all practical purposes with the observed data as shown in Fig. 11.

For the reason mentioned above, we concluded that the numericcal solution obtained on MODEL II−4 was within tolerable limits of error and quite sufficient for our purposes. Figs. 12.a−b show the distributions of tidal currents solved on MODEL II−4. We will use the results obtained on MODEL II−4 as the field of tidal currents for water quality analysis.

c. The rate of seawater exchange in Fukaura-wan

The rate of seawater exchange was calculated using the following difinition

$$r = \int_0^T Q_{in}\, dt / V_l \qquad (9)$$

where Q_{in} is the tidal discharge of inflow through a cross section (m^3/sec), V_l the water volume at low tide (m^3), and

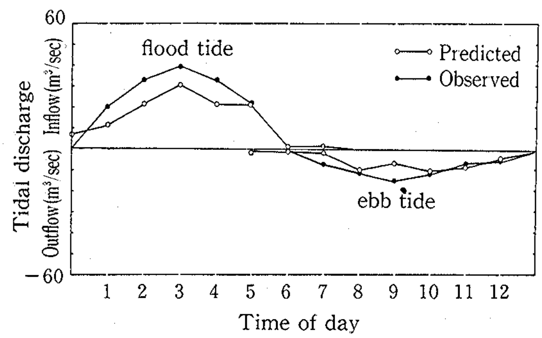

Fig 11. Comparison of tidal discharge predicted with that observed at Stn. 4.

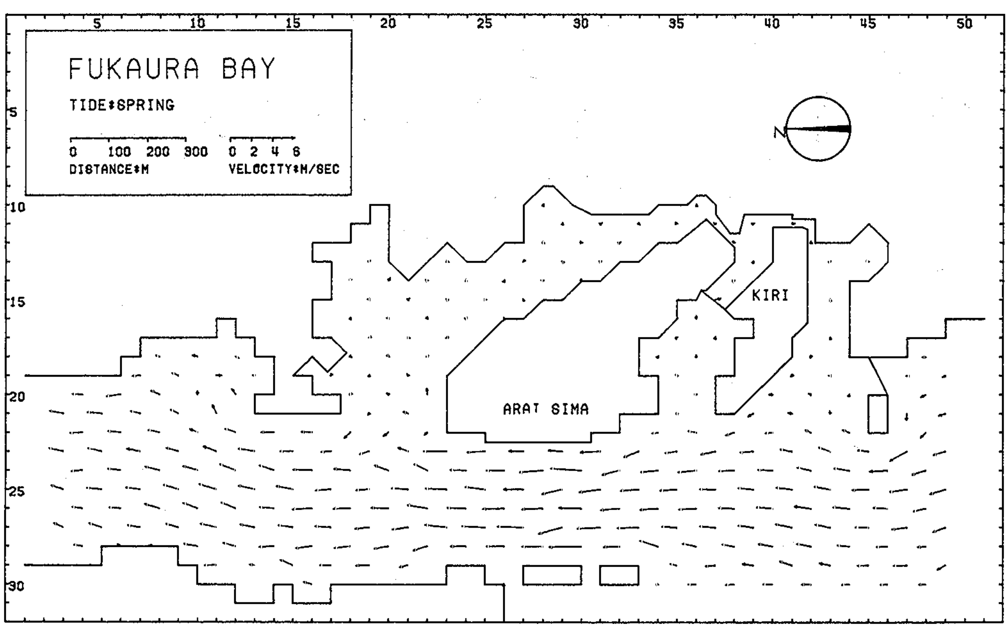

Fig 12 a. Distribution of maximum tidal currents at spring flood tide.

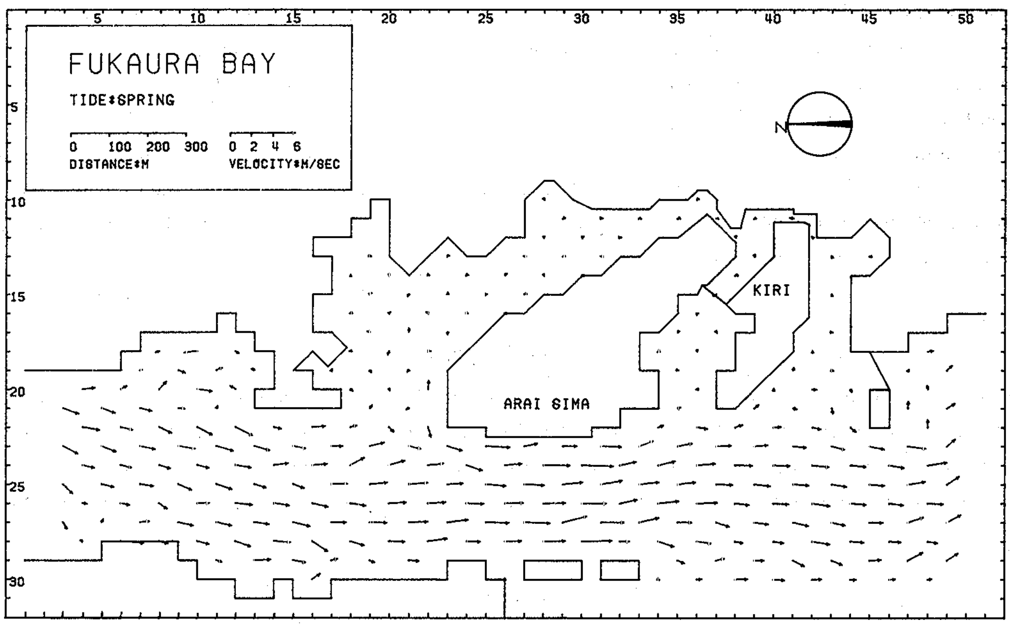

Fig 12.b Distribution of maximum tidal currents at spring ebb tide.

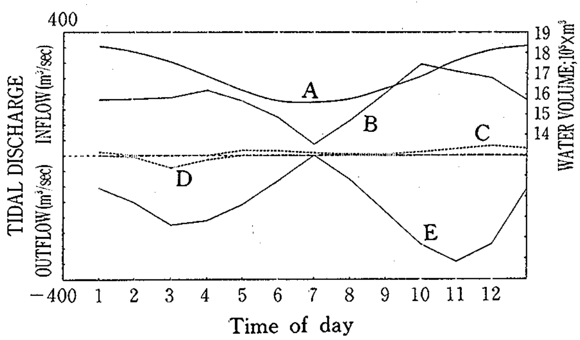

Fig. 13. Variations in tidal discharge and water volume in Fukaura-wan.
A: Water volume, B and E: Inflow and outflow through the northern mouth, C and D: Inflow and outflow through the narrow channel.

Table 3. Hydraulic characteristics in Fukaura-wan

Water area, m^2	Water Volume, m^3			Volume of inflow	Volume of outflow	Exchange rate
	L. W. V_L	H. W. V_H	V_H/V_L	Q_{in} m^3/12hr	Q_{out} m^3/12hr	Q_{in}/V_l 1/12hr
24.5×10^4	160×10^4	183×10^4	1.2	871×10^4	813×10^4	5.6

T the tidal period (hrs).

$$Q=\sum_{i=1}^{n} A_i|V|_i,\quad A=\sum_{i=1}^{n} \Delta s H_{i,j}^{t},\quad V=[(U_{i,j}^{t})^2+(V_{i,j}^{t})^2]^{\frac{1}{2}}\cos\phi$$

where A is the cross sectional area, Δs the grid interval, H the total water depth at the grid point (i, j), V the velocity at grid point normal to the vertical cross section, ψ the angle between the computed velocity vector and the velocity normal to the cross section, and $U^t_{i,j}$, $V^t_{i,j}$ are the velocities obtained on MODEL II−4. $V>0$; inflow, $V<0$; outflow, n; the number of cross-section divided

Changes in disharge and water volume are summarized as shown in Fig. 13 and Table 3. It may be found that as the volume of inflow from the northern mouth is Q_{in} and water volume at low water is V_l, the exchange rate of sea water Q_{in}/V_l is 5.6/12 hrs. This means that about 77% of the volume of the bay water at low water is replaced with open sea water through the northern bay mouth in one tide cycle.

Acknowledgments

This work was supported by the Nagasaki Fishery Experimental Station, Nagasaki-ken. The data analysis in the present paper was carried out on a MELCOM-COSMO-700S in the data station of Kagawa University. The authors wish to thank the scientists and the staffs of these stations for helping in the field surveys and the data analysis. The authors also would like to thank Mr. Yoshihiko Tsuruta, a graduate student, for his cooperation in this study.

References

(1) SASAKI, T and INOUE, H.: Tec. Bull. Fac. Agr. Kagawa Univ. Vol. 37, No. 1, 41−53 (1985).

(2) SASAKI, T., POTAPIROM, T. and INOUE, H.: Tec. Bull. Fac. Agr. Kagawa Univ. Vol 37, No. 2, 131−148 (1986).

(3) TAMURA, T.: Fisheries engineering, Tokyo, Chizin-shokan (1968)

(4) MILINE, P. H.: Tidal Current Forces on Mesh Netting, Fisheries news LTD (1972).

(Received May 31, 1986)